

**CONTROL OF CHEMOTACTIC SIGNAL GAIN
VIA MODULATION OF A PRE-FORMED RECEPTOR ARRAY***
Hiroki Irieda¹, Motohiro Homma^{1§}, Michio Homma¹, and Ikuro Kawagishi^{1,2}
**From ¹Division of Biological Science, Graduate School of Science, and ²Institute for
Advanced Research, Nagoya University, Chikusa-ku, Nagoya 464-8602, Japan**

Running title: Bacterial chemoreceptor array

Address correspondence to: Ikuro Kawagishi, Division of Biological Science, Graduate School of Science, Nagoya University, Chikusa-ku, Nagoya 464-8602, Japan, Tel, +81 52-789-2993; Fax, +81 52-789-3001; E-mail, i45406a@cc.nagoya-u.ac.jp

[§]Present address: Department of Life Sciences, Graduate School of Arts and Sciences, University of Tokyo, 3-8-1 Komaba, Meguro, Tokyo 153-8902, Japan.

The remarkably wide dynamic range of the chemotactic pathway of *Escherichia coli*, a model signal transduction system, is achieved by methylation/amidation of the transmembrane chemoreceptors, which regulate the histidine kinase CheA in response to extracellular stimuli. The chemoreceptors cluster at a cell pole together with CheA and the adaptor CheW. Several lines of evidence have led to models that assume high cooperativity and sensitivity via collaboration of receptor dimers within a cluster. Here, using *in vivo* disulfide crosslinking assays, we demonstrate a well-defined arrangement of the aspartate chemoreceptor (Tar). The differential effects of amidation on crosslinking at different positions indicate that amidation alters the relative orientation of Tar dimers to each other (presumably inducing rotational displacements) without much affecting the conformation of the periplasmic domains. Interestingly, the effect of aspartate on crosslinking at any position tested was roughly opposite to that of receptor amidation. Furthermore, amidation attenuated the effects of aspartate by several orders of magnitude. These results suggest that receptor covalent modification controls signal gain by altering the arrangement or packing of receptor dimers in a pre-formed cluster.

Chemotaxis of *Escherichia coli* is one of the most extensively studied sensory systems, recognizing the concentration of environmental chemicals and migrating toward the favorite direction (for reviews, see 1-5). All of the components have been identified and extensively studied. However, the molecular mechanisms

underlying its high sensitivity and wide dynamic range have not been fully understood. The chemotactic signal is transmitted from the chemoreceptors to the flagellar motor via a stoichiometric His-Asp phosphorelay from the histidine kinase CheA to the response regulator CheY. The chemoreceptors of *Escherichia coli* belong to one of the best studied transmembrane receptor families. The receptor cytoplasmic domain interacts with CheA and the adaptor protein CheW (6, 7) and the resulting ternary complexes form a cluster at a cell pole (8-10). Attractant binding to the Tar dimer, which is formed regardless of its ligand occupancy state (11), induces a small but critical inward displacement of a membrane-spanning α -helix of one subunit (12-17). This displacement is thought to trigger a structural change in the cytoplasmic domain, which then inactivates CheA. To account for high sensitivity of the chemotaxis system, however, it has been proposed that attractant binding also affects neighboring receptor dimer(s) (18-21), models which have been supported by several lines of evidence (21-26). Receptor clustering has also been implicated in signal gain control by methylation (or amidation) of specific glutamate residues that is responsible for adaptation to persisting stimuli. Only a slight decrease in the attractant-binding affinity (27-30) and a slight increase in the CheA activity (28, 30) that result from receptor covalent modification cannot account for adaptation. Rather, receptor methylation/amidation seems to control signal gain presumably through receptor clustering (21, 23, 30). However, receptor methylation/amidation does not drastically alter the polar localization of the high-abundance chemoreceptors (31-33).

We have already established, by using a site-directed disulfide crosslinking assay, that receptor dimers interact with each other *in vivo* and that this interaction is modulated by attractant binding (26). Here, we employed this technique to ask whether receptor clustering is involved in gain control. Systematic disulfide scanning revealed a well-defined array of receptor dimers. Crosslinking at different positions were affected differentially by receptor amidation (equivalent to methylation), suggesting that receptor amidation alters relative orientation of receptor dimers in the cluster rather than inducing their association or dissociation. In any position tested, attractant binding showed effects roughly opposite to amidation but these attractant effects were attenuated by increasing levels of amidation. These results suggest that receptor amidation (methylation) controls signal gain by altering the arrangement or packing of receptor dimers in a pre-formed cluster.

Experimental Procedures

Bacterial strains and plasmids—Strain HCB339 (34) lacks all four chemoreceptors, whereas strain HCB436 (35) lacks all four chemoreceptors, CheB, and CheR. All Tar-encoding plasmids used for the crosslinking assays were derived from pWSK29 (36), a derivative of pSC101 that carries the *bla* gene. Site-directed mutagenesis of *tar* was carried out essentially as described previously (26).

Swarm assay of chemotaxis—Swarm assays were performed with tryptone semisolid agar (1% tryptone, 0.5% NaCl, 0.3% agar) supplemented with 50 mg/ml ampicillin. After swarm plates were inoculated with fresh colonies, they were incubated at 30°C for 10 to 20 h. In some experiments, cell suspensions were spotted onto a plate, which was then incubated at 30°C for 8 to 9 h.

In vivo disulfide crosslinking—Disulfide crosslinking and immunoblotting were essentially as described previously (26). TG broth [1% tryptone, 0.5% NaCl, 0.5% (w/v) glycerol] supplemented with 50 mg/ml ampicillin was inoculated at 1:30 dilution with a fresh overnight culture of cells carrying a plasmid. Cultures were then shaken at 30°C. After 3.5 h, cells were

harvested and suspended in SDS-loading buffer [35 mM Tris-HCl (pH 6.8), 6.7% glycerol, 1% SDS, 0.0007% BPB] supplemented with 2.5 mM NEM and 2.5 mM EDTA. When necessary, 2ME was added to the final concentration of 12.5%. Samples were transferred onto a polyvinylidene difluoride membrane (Millipore Japan, Tokyo) using a semidry blotting apparatus (Biocraft, Tokyo). The antibody raised against the C-terminal peptide [NH₂-(C)PRLRIAEQDPNWETF-COOH] of Tar (α Tar-C) was prepared by Sawadi Technology Co. (Tokyo). The HRP-linked anti-rabbit IgG antibody (Cell Signaling Technology, Beverly, MA, U.S.A.) was used as the second antibody. The protein-antibody complexes were visualized with ECL Western-blotting detection reagents (Amersham Pharmacia Biotech).

To quantify the intensity of the Tar band, the immunoblots were scanned and the resulting images were analyzed by using the software ImageJ (<http://rsb.info.nih.gov/ij/>). The crosslinking efficiency (in percentage) of a given Tar mutant protein was defined as a proportion of the crosslinked dimers to the total amount. For each mutant, crosslinking assays were triplicated with three independent transformants and the mean and standard deviation values were calculated.

To examine the effects of an attractant on disulfide crosslinking, cells were grown for 3.5 h as described above, washed twice with EDTA-free MLM medium [10 mM potassium phosphate buffer (pH 7.0), 10 mM DL-lactate, 0.1 mM methionine], resuspended in EDTA-free MLM, and divided into aliquots. MeAsp ($0\text{-}10^{-3}$ M) was added to each aliquot. The samples were incubated for 10 min at room temperature or at 30°C, before being treated with an oxidizing catalyst Cu(II)(*o*-phenanthroline)₃ (hereafter referred to as Cu-phenanthroline) (0-200 μ M) supplemented with MeAsp ($0\text{-}10^{-3}$ M) for 10 min at room temperature or at 30°C. To stop the oxidation reaction, 1/5 volume of prechilled stop solution [210 mM Tris-HCl (pH 6.8), 15 mM EDTA, 15 mM NEM] supplemented with MeAsp ($0\text{-}10^{-3}$ M) was added to the samples and then samples were put on ice. Cells were collected and suspended in SDS-loading buffer containing 2.5 mM NEM and 2.5 mM EDTA supplemented

with MeAsp ($0\text{-}10^{-3}$ M). When necessary, 2ME was added. Samples were analyzed by immunoblotting as described above.

Results

Receptor dimers are organized into a well-defined array—To probe the relative orientation of receptor dimers in a polar cluster, we systematically introduced Cys residues within or near loop 2-3 of the periplasmic domain of the aspartate chemoreceptor Tar (Fig. 1). The loop sticks out from the dimer in the crystal and might constitute an interdimer contact surface. The resulting proteins were expressed in HCB339 cells, which lack all receptors, at levels similar to that of chromosome-encoded wild-type Tar (data not shown). Cells expressing any mutant Tar except Tar-A118C, which caused growth retardation, swarmed as fast as those expressing wild-type Tar (data not shown), indicating that the Cys substitutions, except A118C, by themselves do not severely affect receptor function.

To avoid any complexity from covalent modification, the mutant proteins were then expressed in HCB436 cells, which lack all receptors, the methyltransferase CheB, and the methyltransferase CheR. Immunoblotting revealed that all of them formed crosslinked dimers in the presence of Cu-phenanthroline *in vivo* (data not shown), which are deduced to result from crosslinking between native dimers since the double mutants with S36C (located at the subunit interface within a dimer) yielded crosslinked oligomers in the presence of Cu-phenanthroline (data not shown). In the absence of Cu-phenanthroline, the crosslinking efficiencies at positions in helix 3 (A118C-I123C) exhibited a periodicity that is consistent with the water-accessibility of an α -helix packed against the rest of the protein (12, 37) (Fig. 2A, C). The variation of the mobility of the dimers on the SDS-PAGE gels should be due to their shape: the closer the crosslinking point to the midpoint of the molecule, the slower the crosslinked dimer would migrate in the gel matrix. Along with the dependence of interdimer crosslinking on the presence of CheA and CheW (data not shown and ref. 26), this pattern supports the idea that the *in vivo* interdimer crosslinking of Tar reflects its

native structure. The Cys residues in the C-terminal half of loop 2-3 (P114C-V117C) were more apt to be crosslinked than those in the N-terminal half (K108C-L113C), indicating that in the receptor clusters, the former positions are more closely located to each other. A very high crosslinking efficiency at position 118 might account for the failure of the A118C protein to support swarming of HCB339 cells. When combined with the S36C mutation, all of the resulting double Cys mutant proteins yielded crosslinked oligomers as has been shown for the S36C&D142C protein (26), demonstrating that all these disulfides in or near the loop crosslink subunits from different dimers. Prolonged incubation of the double Cys-mutant protein S36C&D142C with Cu-phenanthroline resulted in accumulation of the deduced hexamer over the other oligomers (Fig. 2B). In contrast, the S36C&M116C protein did not exhibit such a pattern.

On the basis of the efficiencies of crosslinking and the assumption of a “trimer of dimers” unit (24, 38-40), we propose a relative arrangement of three Tar dimers in a receptor array (Fig. 3). This model, albeit being only qualitative without precise distance and orientation, can predict the differential patterns of crosslinked oligomers. The S36C&D142C protein would allow the formation of disulfide bonds between all six subunits in the model, whereas the S36C&M116C protein cannot form a crosslinked hexamer: only two Cys residues of the three “inner” subunits can be crosslinked. *Differential effects of receptor amidation on crosslinking at various positions.*—To examine the effect of covalent modification on the arrangement of receptor dimers in a cluster, we introduced mutations into the four methylation sites, Gln295, Glu302, Gln309 and Glu491 (collectively referred to as QEQE), of each Cys-replaced Tar to yield three amidation states: fully deamidated (EEEE), intermediate (QEQE) and fully amidated (QQQQ) (Fig. 1). It has been established that a Gln residue mimics a methylated Glu residue (27, 28) and that receptor methylation (amidation) increases the mobility of the protein in SDS-PAGE. The representative gel is shown in Fig. 4, demonstrating that amidation has different effects on crosslinking at

different positions. It should be noted that both the concentration of Cu-phenanthroline and the amount of protein were optimized for each Cys position to detect differences among the differentially amidated variants. The assay was triplicated and the crosslinking efficiencies were quantified (Fig. 4B). The Cys residues showed different patterns, which can be divided into three classes: the efficiency of crosslinking at a given position was highest at the (i) QQQQ, (ii) EEEE or (iii) QEQE state, whereas crosslinking at S36C was not detectably changed. The results are summarized by color-coded positions in the three-dimensional structure of Tar (Fig. 5).

The positions showing similar effects of methylation (class i, ii or iii) tend to cluster in the three-dimensional structure, lining up along the long axis (Fig. 5). Since an efficiency of disulfide formation at a given position is highly sensitive to the distance between two thiol groups, the simplest model to account for the pattern may be that receptor amidation (methylation) induces slight rotational movement of Tar dimers either around the axis of symmetry of the dimer (Fig. 6A) or the "trimer of dimers" (Fig. 6B). Since receptor methylation does not affect crosslinking at the cytoplasmic trimer contact (25), it is necessary to assume a twist at somewhere between the cytoplasmic trimer contact and the transmembrane region in the former model. Such a twist might occur within the structurally undefined HAMP domain, which connects the second transmembrane to the first methylation helix. The latter model does not require any twist within a dimer but involves a larger movement.

Effects of attractant binding oppose those of amidation—We also examined the effect of α -methyl-DL-aspartate (MeAsp), a non-metabolizable analog of aspartate, on interdimer crosslinking. It has already been shown that MeAsp does not affect intradimer crosslinking at S36C but decreases interdimer crosslinking at D142C without any detectable change in receptor localization (26), although, on a longer time scale, the addition of an attractant decreases receptor localization (41). We found that MeAsp either increases (S109C and P112C) or decreases (N122C) interdimer crosslinking depending on the position of the introduced Cys

(Fig. 7). For any mutant tested, the effect of MeAsp on crosslinking was roughly opposite to that of receptor methylation. The reciprocal effects of attractant and methylation are consistent with previous two-state models of receptor signaling and adaptation (42-45).

Receptor amidation attenuated attractant effects on crosslinking—To examine whether the dimer-to-dimer interaction of Tar is involved in gain control by covalent modification, we examined the effect of the MeAsp concentration on interdimer crosslinking. The representative results are shown in Fig. 8. In this assay, variations were too high to quantify the crosslinking efficiencies, but the results were qualitatively reproducible. For N122C, the threshold concentration of MeAsp for decreasing crosslinking of the EEEE form was at least 10^3 -fold higher than that for the QQQQ form. Similar results were obtained for D142C (data not shown). By contrast, the EEEE form of the P112C mutant was crosslinked even in the absence of MeAsp at an efficiency similar to that in the presence of saturating concentrations of MeAsp, presumably because the fully demethylated state mimics attractant binding at least to some extent, while crosslinking of the QQQQ form was increased only in the presence of 1 mM MeAsp. Similar results were obtained for S109C (data not shown). Thus, the aspartate effects (regardless of polarity) on interdimer crosslinking are attenuated by covalent modification (amidation) of Tar, suggesting that gain control by covalent modification of the chemoreceptor involves modulation of arrangement or packing of the receptor array.

Discussion

The structures of the intact chemoreceptors, the intact kinase CheA, and their complex with the adaptor CheW remain unresolved, which has impeded understanding of the mechanisms of signaling through the chemoreceptor-CheW-CheA cluster. The systematic disulfide crosslinking assays presented in this study have led to the following key findings about chemoreceptor clustering and its physiological significance: (i) chemoreceptor dimers are organized into a well-defined array in *E. coli* cells; (ii) receptor

amidation and attractant binding have roughly opposite effects on the arrangement, packing and/or dynamics of receptor dimers within the array; and (iii) increasing levels of amidation attenuate effects of attractant binding, hence presumably decreasing signal gain (Fig. 9). In essence, the receptor array is in an equilibrium between the kinase ON and OFF states, which are favored by methylation (amidation) and attractant binding, respectively. We propose that receptor methylation controls signal gain by rearranging receptor dimers (*e.g.* inducing a small rotational displacement) with a polarity opposite to attractant binding and restricting the attractant-induced rearrangement of receptor dimers.

It has recently been shown that receptor methylation (amidation) slightly increases its polar localization (31-33). Although such a small increase cannot account for adaptation, amidation would enhance interdimer crosslinking at all positions. The differential effects on crosslinking at various positions argue that enhanced localization or clustering is not a major effect of receptor amidation but that it alters the arrangement or packing of dimers within a

pre-formed cluster. By contrast, crosslinking of receptor dimers at the cytoplasmic "trimer contact" is not affected by receptor amidation or even by the presence or absence of CheA and CheW (24, 25). We therefore suspect that the proposed arrangement (Fig. 3) represents three dimers from neighboring "trimer of dimers" units rather than from within a single unit, which is consistent with previous models that assume a well-defined receptor array (40).

Methylation may also modulate structural dynamics of the receptor. In fact, the addition of MeAsp induced little change in crosslinking of the EEEE forms of the S109C and P112C proteins. This result is consistent with the suggestion that the unmodified chemoreceptor is more dynamic than the amidated one (40). It remains unclear how the rearrangement of receptor dimers can regulate the CheA kinase activity. Nevertheless, our results shed new light on the significance of receptor clustering or receptor quaternary structures in signal transduction. Moreover, the crosslinking technique may be applied to isolate receptor oligomers or larger clusters for structural studies.

REFERENCES

1. Blair, D. F. (1995) *Annu. Rev. Microbiol.* **49**, 489-522
2. Falke, J. J., Bass, R. B., Butler, S. L., Chervitz, S. A. & Danielson, M. A. (1997) *Annu. Rev. Cell Dev. Biol.* **13**, 457-512
3. Stock, J. B. & Levit, M. (2000) *Curr. Biol.* **10**, R11-R14
4. Bourret, R. B. & Stock, A. M. (2002) *J. Biol. Chem.* **277**, 9625-9628
5. Sourjik, V. (2004) *Trends Microbiol.* **12**, 569-576
6. Gegner, J. A., Graham, D. R., Roth, A. F. & Dahlquist, F. W. (1992) *Cell* **70**, 975-982
7. Schuster, S. C., Swanson, R. V., Alex, L. A., Bourret, R. B. & Simon, M. I. (1993) *Nature* **365**, 343-347
8. Maddock, J. R. & Shapiro, L. (1993) *Science* **259**, 1717-1723
9. Skidmore, J. M., Ellefson, D. D., McNamara, B. P., Couto, M. M., Wolfe, A. J. & Maddock, J. R. (2000) *J. Bacteriol.* **182**, 967-973
10. Sourjik, V. & Berg, H. C. (2000) *Mol. Microbiol.* **37**, 740-51
11. Milligan, D. L. & Koshland, D. E. Jr. (1988) *J. Biol. Chem.* **263**, 6268-6275
12. Milburn, M. V., Prive, G. G., Milligan, D. L., Scott, W. G., Yeh, J., Jacarik, J., Koshland, D. E. Jr. & Kim, S. H. (1991) *Science* **254**, 1342-1347
13. Chervitz, S. A., Lin, C. M. & Falke, J. J. (1995) *Biochemistry* **34**, 9722-9733
14. Chervitz, S. A. & Falke, J. J. (1995) *J. Biol. Chem.* **270**, 24043-24053
15. Chervitz, S. A. & Falke, J. J. (1996) *Proc. Natl. Acad. Sci. USA* **93**, 2545-2550
16. Ottemann, K. M., Xiao, W., Shin, Y. K. & Koshland, D. E. Jr. (1999) *Science* **285**, 1751-1754
17. Falke, J. J. & Hazelbauer, G. L. (2001) *Trends Biochem. Sci.* **26**, 257-265

18. Bray, D., Levin, M. D. & Morton-Firth, C. J. (1998) *Nature* **393**, 85-88
19. Duke, T. A. & Bray, D. (1999) *Proc. Natl. Acad. Sci. USA* **96**, 10104-10108
20. Mello, B. A. & Tu, Y. (2003) *Proc. Natl. Acad. Sci. USA* **100**, 8223-8228
21. Sourjik, V. & Berg, H. C. (2004) *Nature* **428**, 437-441
22. Gestwicki, J. E. & Kiessling, L. L. (2002) *Nature* **415**, 81-84
23. Sourjik, V. & Berg, H. C. (2002) *Proc. Natl. Acad. Sci. USA* **99**, 123-127
24. Ames, P., Studdert, C. A., Reiser, R. H. & Parkinson, J. S. (2002) *Proc. Natl. Acad. Sci. USA* **99**, 7060-7065
25. Studdert, C. A. & Parkinson, J. S. (2004) *Proc. Natl. Acad. Sci. USA* **101**, 2117-2122
26. Homma, M., Shiomi, D., Homma, M. & Kawagishi, I. (2004) *Proc. Natl. Acad. Sci. USA* **101**, 3462-3467
27. Dunten, P. & Koshland, D. E. Jr. (1991) *J. Biol. Chem.* **266**, 1491-1496
28. Borkovich, K. A., Alex, L. A. & Simon, M. I. (1992) *Proc. Natl. Acad. Sci. USA* **89**, 6756-6760
29. Iwama, T., Homma, M. & Kawagishi, I. (1997) *J. Biol. Chem.* **272**, 13810-13815
30. Levit, M. N. & Stock, J. B. (2002) *J. Biol. Chem.* **277**, 36760-36765
31. Liberman, L., Berg, H. C. & Sourjik, V. (2004) *J. Bacteriol.* **186**, 6643-6646
32. Lybarger, S. R., Nair, U., Lilly, A. A., Hazelbauer, G. L. & Maddock, J. R. (2005) *Mol. Microbiol.* **56**, 1078-1086
33. Shiomi, D., Banno, S., Homma, M. & Kawagishi, I. (2005) *J. Bacteriol.* **187**, 7647-7654
34. Wolfe, A. J., Conley, M. P., Kramer, T. J. & Berg, H. C. (1987) *J. Bacteriol.* **169**, 1878-1885
35. Wolfe, A. J. & Berg, H. C. (1989) *Proc. Natl. Acad. Sci. USA* **86**, 6973-6977
36. Wang, R. F. & Kushner, S. R. (1991) *Gene* **100**, 195-199
37. Yeh, J. I., Biemann, H. P., Prive, G. G., Pandit, J., Koshland, D. E. Jr. & Kim, S. H. (1996) *J. Mol. Biol.* **262**, 186-201
38. Kim, K. K., Yokota, H. & Kim, S. H. (1999) *Nature* **400**, 787-792
39. Shimizu, T. S., Le Novere, N., Levin, M. D., Beavil, A. J., Sutton, B. J. & Bray, D. (2000) *Nat. Cell Biol.* **2**, 792-796
40. Kim, S. H., Wang, W. & Kim K. K. (2002) *Proc. Natl. Acad. Sci. USA* **99**, 11611-11615
41. Inoue, I., Shiomi, D., Kawagishi, I. & Yasuda, K. (2004) *J. Nanobiotech.* **2**, 4-8
42. Asakura, S., & Honda, H. (1984) *J. Mol. Biol.* **176**, 349-367
43. Barkai, N. & Leibler, S. (1997) *Nature* **387**, 913-917
44. Morton-Firth, C. J., Shimizu, T. S. & Bray, D. (1999) *J. Mol. Biol.* **286**, 1059-1074
45. Bornhorst, J. A. & Falke, J. J. (2003) *J. Mol. Biol.* **326**, 1597-1614

FOOTNOTES

*We thank Toshiharu Yakushi for helpful discussion and encouragement. This work was supported in part by grants-in-aid for scientific research to I. K. from the Japan Society for the Promotion of Science and from the Institute for Advanced Research, Nagoya University.

The abbreviations used are: Cu-phenanthroline, Cu(II)(*o*-phenanthroline)₃; EDTA, ethylenediaminetetraacetic acid; 2ME, 2-mercaptoethanol; NEM, *N*-ethylmaleimide

FIGURE LEGENDS

Fig. 1. Disulfide scanning of the periplasmic domain of the aspartate chemoreceptor Tar. *A*, The three-dimensional structure of the periplasmic fragment of *Salmonella* Tar (12). Residues replaced by Cys are marked by balls. *B*, A schematic illustration of the positions of the introduced Cys residues. Wild-type Tar is devoid of Cys residues. Residues (K108-I123) within or near loop 2-3, a potential interdimer interface, were systematically replaced by Cys. Substitutions of residue S36 at the subunit interface within the Tar dimer and residues D142, Y143 and G144 at the external surface of the dimer

were described previously (26). Filled circles indicate the four methylation sites (Q295, E302, Q309, and E491). H, L and TM denote α -helices, loops and transmembrane helices, respectively. Although the cytoplasmic domain of Tar is larger than the periplasmic domain, it has been simply represented by a single box in the diagram.

Fig. 2. Detection of *in vivo* disulfide-crosslinked products of Cys-replaced Tar proteins. *A, B*, Single Cys mutant proteins (*A*) and double Cys mutant proteins (*B*) were expressed in HCB436 cells and detected by immunoblotting. Crosslinking of the single Cys mutant proteins was examined in the absence of Cu-phenanthroline, whereas cells expressing the S36C&D142C or S36C&M116C protein were incubated for 15 or 20 minutes in the presence of Cu-phenanthroline. *C*, Quantification of the crosslinking efficiencies of the single Cys mutant proteins. The crosslinking efficiency (in percentage) of a given Tar mutant protein was defined as a proportion of the crosslinked dimers to the total amount. Crosslinking assays were at least triplicated with independent transformants, resulting in consistent patterns with varied absolute crosslinking efficiencies. Shown here is the representative result.

Fig. 3. Proposed arrangement of three Tar dimers in a receptor array. The green balls denote the positions of the Cys substitutions. Position 36 is located at the subunit interface within the Tar dimer, whereas the other substitutions were made on the external surface of the dimer. The more deeply shaded balls indicate positions at which a higher efficiency of crosslinking was observed. Left panel: top view (*i.e.* looking down from the outer membrane); right panel: bottom view (*i.e.* looking up from the cytoplasm).

Fig. 4. Differential effects of receptor modification on interdimer crosslinking at different positions. *A*, Detection of crosslinked dimers of the three different amidation variants (EEEE: 4E, QEQE: QE, QQQQ: 4Q) of each Cys-carrying mutant protein. Both the concentration of Cu-phenanthroline and the amount of protein were optimized for each Cys position to detect differences among the differentially amidated variants. Note that amidation increases the mobility of the receptor protein in SDS-PAGE. *B*, Quantification of the crosslinking efficiencies of mutant Tar proteins of the three different amidation variants. The crosslinking efficiency (in percentage) of a given Tar mutant protein was defined as a proportion of the crosslinked dimer (on a non-reducing gel) to the total amount (on a reducing gel). For each mutant, crosslinking assays were triplicated with three independent transformants and the mean and standard deviation values were plotted. The P114C and V117C proteins were not included since each of these mutant proteins yielded two separate bands that can be taken as the crosslinked dimer.

Fig. 5. Classification of the Cys positions with respect to the differential effects of receptor amidation on Cys crosslinking. The Cys residues were placed onto the three-dimensional structure and divided into three classes: the efficiency of crosslinking at a given position was highest when the amidation state of the protein was QQQQ (red), EEEE (blue) or QEQE (magenta). Crosslinking at position 36 (yellow) was not detectably changed by amidation. The P114C and V117C proteins formed two dimer bands, and the positions of the Cys residues have been marked with pink balls. Left top panel: top view; left bottom panel: bottom view; right panel: side view.

Fig. 6. Models for modulation of the arrangement of tar dimers by amidation/methylation. Receptor modification is assumed to induce slight rotational movement around the two-fold symmetry axis of each dimer (*A*) or the symmetry axis of each "trimer of dimers" unit (*B*). The fully deamidated/demethylated (4E) and fully amidated (4Q) states are shown in the left and right panels, respectively. The arrows indicate the direction of rotation induced by amidation/methylation (left panels) or deamidation/demethylation (right panels). Note that the displacements are exaggerated for clarity.

Fig. 7. Differential effects of MeAsp on interdimer crosslinking at various positions. MeAsp (1 mM)

increased (S109C, P112C) or decreased (N122C, D142C) the formation of crosslinked Tar dimers in HCB436 cells. Note that the intermediate (QE) variants of the proteins were used in these assays. The optimal concentration of Cu-phenanthroline for the detection of the effect of MeAsp was determined for each position.

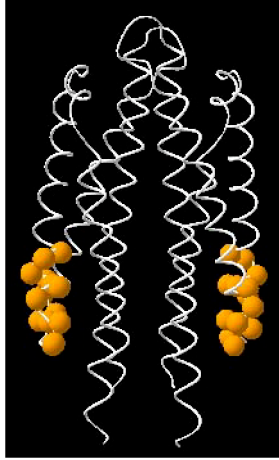
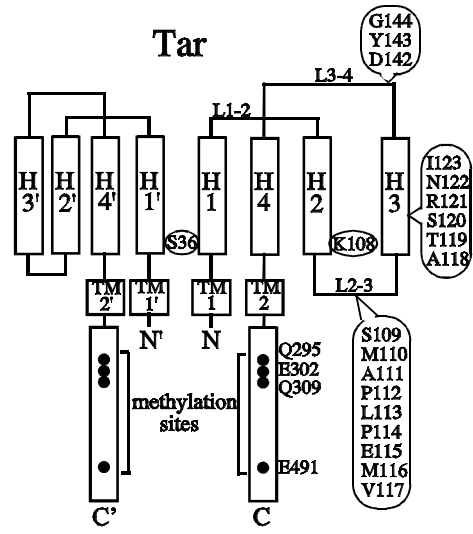
Fig. 8. Attenuation of the effects of MeAsp on interdimer crosslinking by receptor amidation. Crosslinking at P112C and N122C was examined in the presence (200 μ M) and absence of Cu-phenanthroline, respectively.

Fig. 9. A model of gain control by covalent modification of the receptors. At a cell pole, the chemoreceptors forms clusters that are made of "trimer of dimers" units (top panel). Our results demonstrate that these units are organized into a well-defined array (middle panel). Two-state models of the chemoreceptor function assume two extreme states: one activating and the other inactivating CheA (kinase ON and OFF states, respectively). The observed crosslinking is consistent with the notion that methylation (amidation) counteracts attractant binding; attractant binding favors the OFF state, whereas methylation favors the ON state. The results also suggest that receptor methylation restricts the rearrangement (rotation) of the dimers by attractant binding (denoted by the longer light blue arrows for the demethylated state and the shorter arrows for the methylated state), leading to a smaller gain for the same input signal (bottom panel). Higher levels of methylation may also restrict structural fluctuations of the Tar molecule (40).

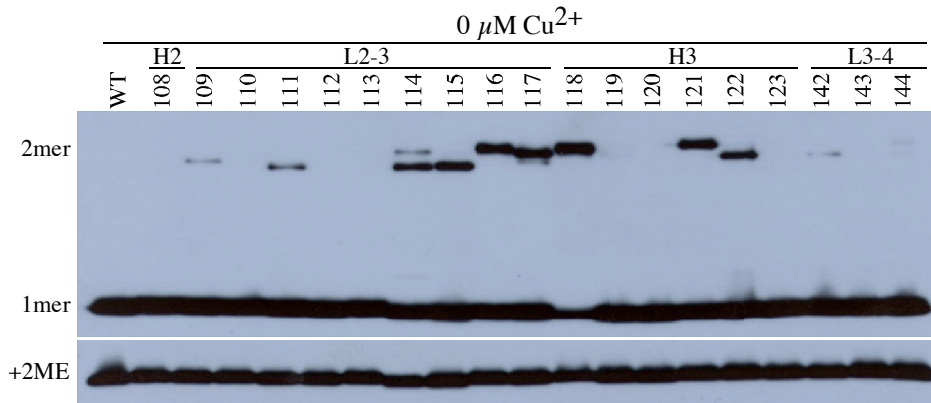
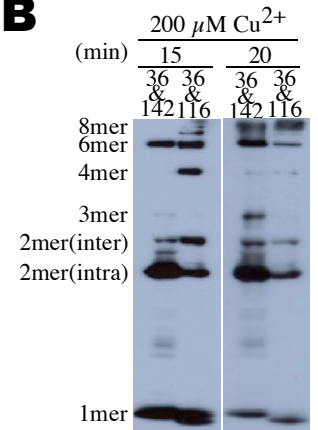
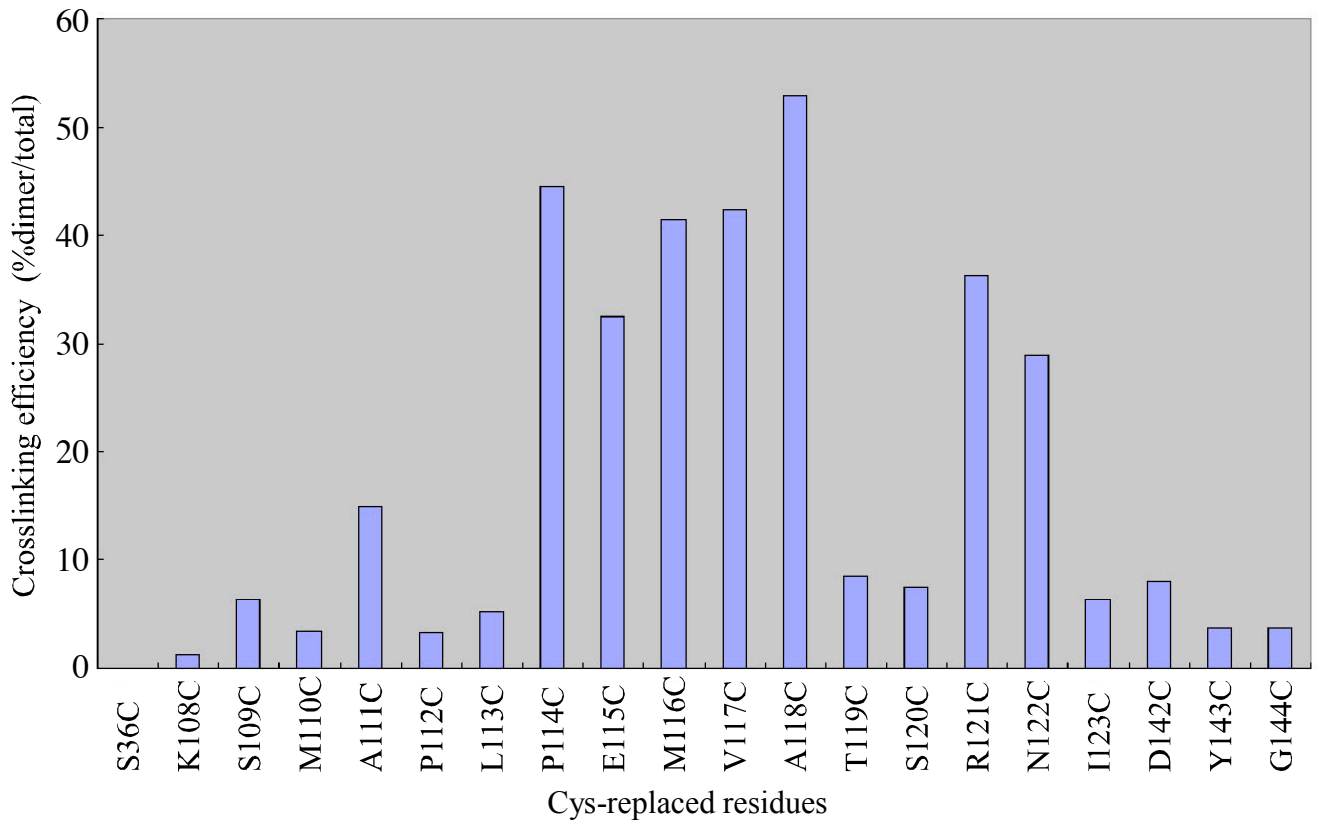
LEGENDS TO SUPPLEMENTAL MATERIALS

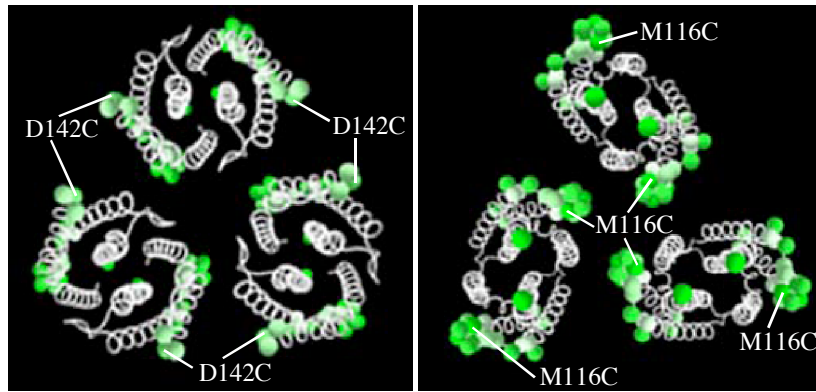
SUPPLEMENTAL VIDEO 1 Animation depicting proposed methylation-induced rotational displacements of chemoreceptor dimers around their symmetry axes. The animation begins with the EEEE state and ends with the QQQQ state. The residues, for which Cys was substituted, are colored as described in the legend to Fig. 5. Note that the displacements are exaggerated for clarity.

SUPPLEMENTAL VIDEO 2 Animation depicting proposed methylation-induced rotational displacements of "trimer of dimers" units of the chemoreceptor around their symmetry axes. The animation begins with the EEEE state and ends with the QQQQ state. The residues, for which Cys was substituted, are colored as described in the legend to Fig. 5. Note that the displacements are exaggerated for clarity.

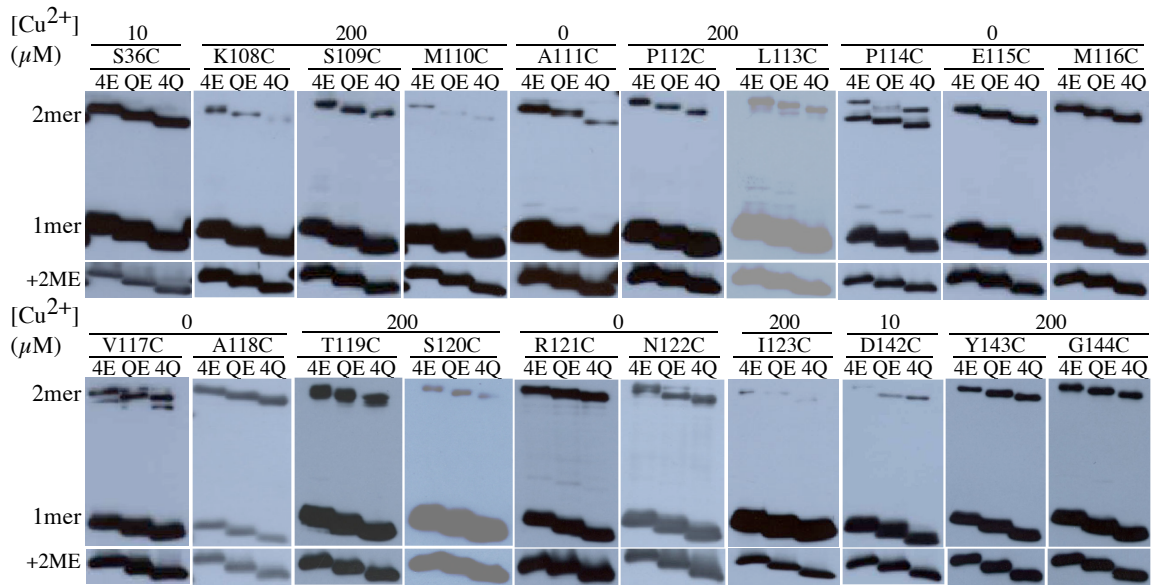
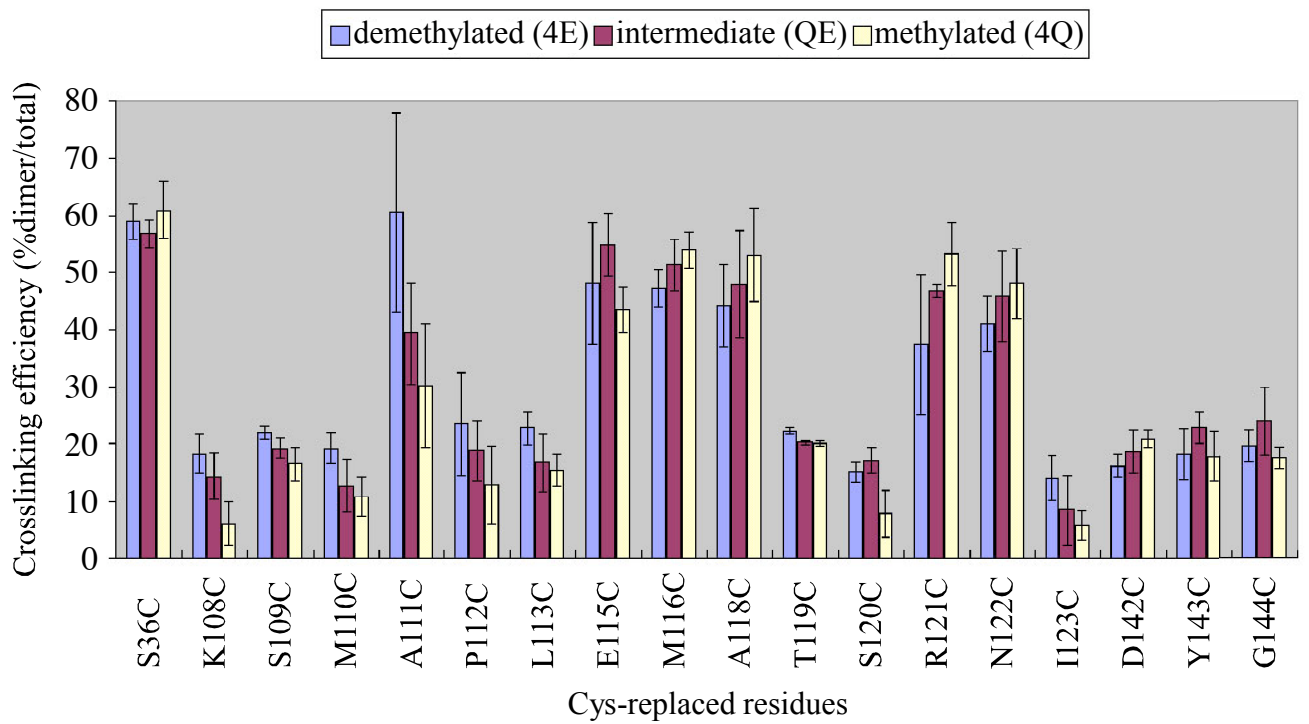
A**B**

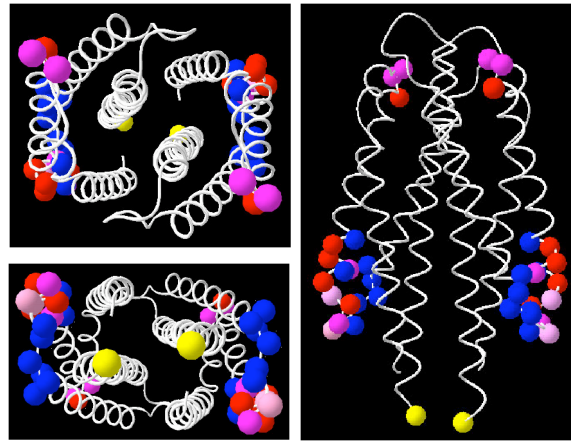
Irieda et al. Fig. 1

A**B****C**

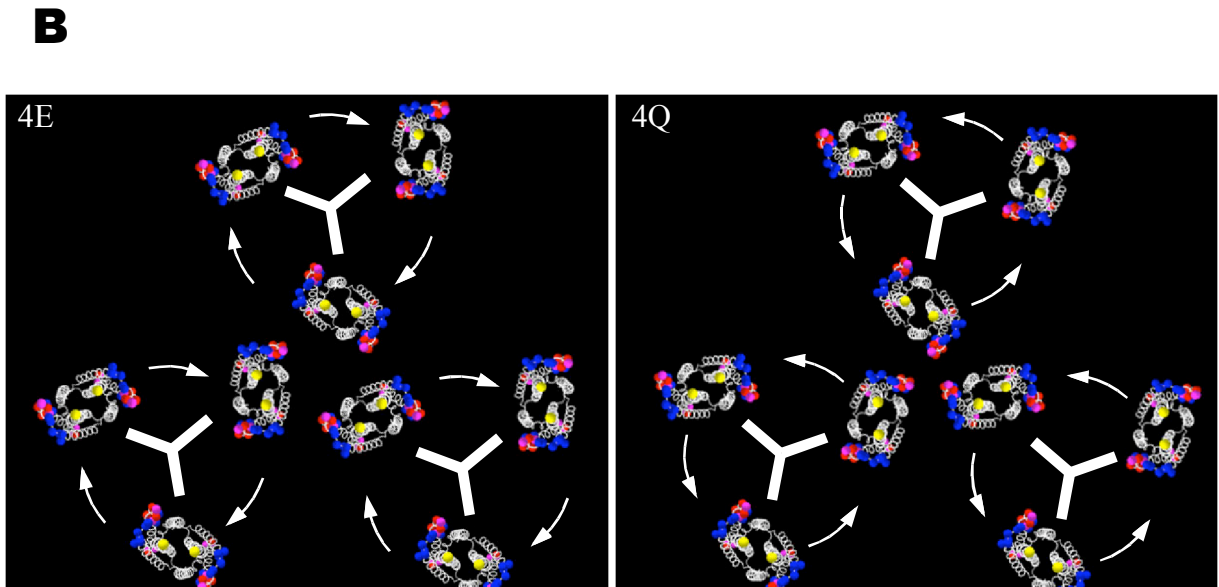
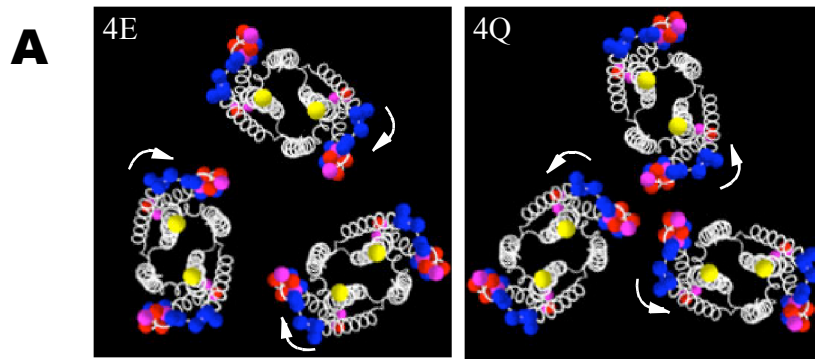


Irieda et al. Fig. 3

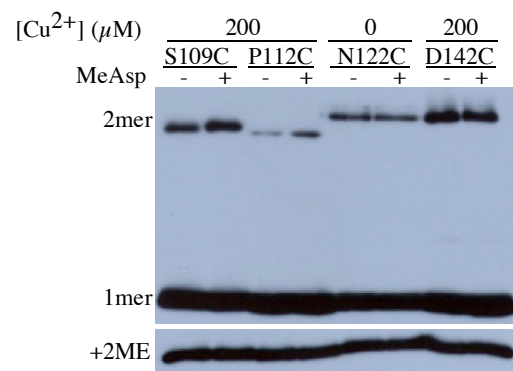
A**B**



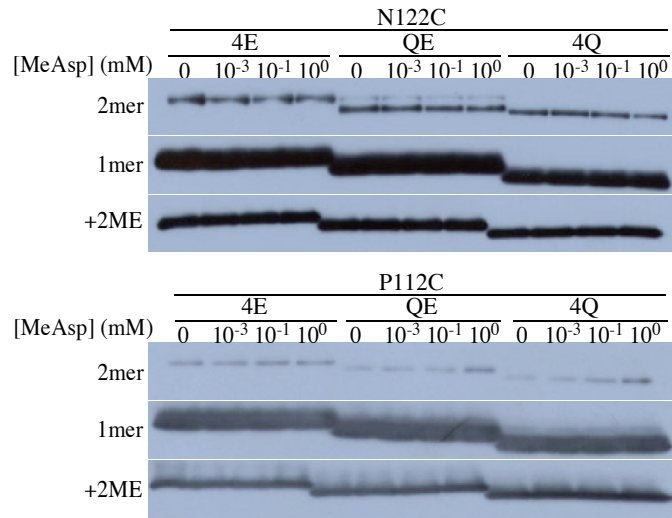
Irieda et al. Fig. 5



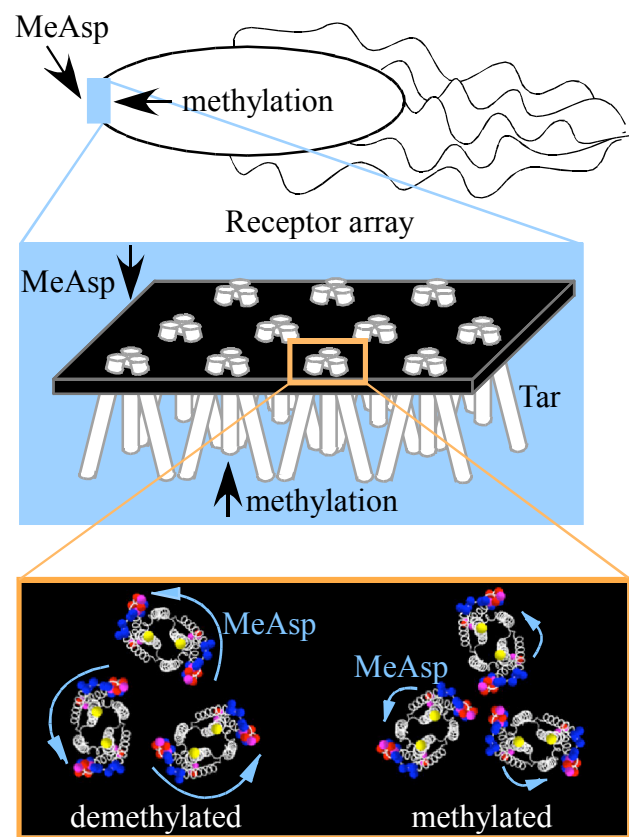
Irieda et al. Fig. 6



Irieda et al. Fig. 7



Irieda et al. Fig. 8



Interface of three "trimer of dimers" units

Irieda et al. Fig. 9